



This is a repository copy of *Furthering the understanding of product formation in monoethanolamine degradation: A mechanistic DFT study*.

White Rose Research Online URL for this paper:

<https://eprints.whiterose.ac.uk/190062/>

Version: Accepted Version

Article:

Parks, C. orcid.org/0000-0001-8016-474X, Hughes, K.J. orcid.org/0000-0002-5273-6998 and Pourkashanian, M. orcid.org/0000-0002-8399-5351 (2022) Furthering the understanding of product formation in monoethanolamine degradation: A mechanistic DFT study. *International Journal of Greenhouse Gas Control*, 119. 103732. ISSN 1750-5836

<https://doi.org/10.1016/j.ijggc.2022.103732>

Article available under the terms of the CC-BY-NC-ND licence (<https://creativecommons.org/licenses/by-nc-nd/4.0/>).

Reuse

This article is distributed under the terms of the Creative Commons Attribution-NonCommercial-NoDerivs (CC BY-NC-ND) licence. This licence only allows you to download this work and share it with others as long as you credit the authors, but you can't change the article in any way or use it commercially. More information and the full terms of the licence here: <https://creativecommons.org/licenses/>

Takedown

If you consider content in White Rose Research Online to be in breach of UK law, please notify us by emailing eprints@whiterose.ac.uk including the URL of the record and the reason for the withdrawal request.



eprints@whiterose.ac.uk
<https://eprints.whiterose.ac.uk/>

1 Furthering the understanding of product formation
2 in monoethanolamine degradation: A mechanistic
3 DFT study.

4 *Christopher Parks*^a, Kevin J. Hughes,^a Mohammed Pourkashanian^a*

5

6 ^a *Department of Mechanical Engineering, The University of Sheffield, Sheffield, S3 7RD, UK*

7

8 *E-mail: c.m.parks@sheffield.ac.uk,*

9 **Abstract**

10

11 A thorough understanding of the product formation originating during degradation of
12 monoethanolamine is crucial to future commercialization of carbon capture plants. Here we
13 report on a series of density functional theory (DFT) calculations outlining chemical pathways
14 for the formation of oxidative degradation products. Fragmentation of monoethanolamine
15 (MEA) radicals is surmountable given standard experimental conditions and can lead to the
16 formation of ethanal, ethanoic acid, ammonia, methylamine, water, formaldehyde, formic acid
17 and imines. Alternatively, the MEA radicals can form hydroperoxides after reaction with
18 oxygen which can subsequently go on to form glycine, glycolic acid and N-(2-
19 hydroxyethyl)glycine (HEGly). Experimentally surmountable routes to the formation of
20 oxazoline, N-(2-hydroxyethyl)ethylenediamine (HEEDA), N,N'-bis(2-
21 hydroxyethyl)ethylenediamine (BHEEDA), epoxides, (2-Methylamino)ethanol (MAE), N-(2-
22 hydroxyethyl)imidazole (HEI) and diethanolamine (DEA) are also presented.

23 **Keywords**

24 DFT; 2-ethanolamine; Mechanistic Pathways; Oxidative and thermal degradation

25 1. Introduction

26

27 The build-up of carbon dioxide (CO₂) in the lower atmosphere is a principal contributor to
28 global warming.¹ The earth's temperature has risen appreciably since the mid-1900s. The
29 demand for electricity worldwide is growing each year and this demand is met in the main by
30 fossil fuel fired power stations. These plants produce significant quantities of CO₂. In 2015,
31 for example, 60 % of the United States' electricity was produced by such plants which
32 contributed 40 % of their annual CO₂ production.² As a consequence of this, there is currently
33 a drive to develop post combustion carbon capture and storage technologies (PCCC) to mitigate
34 the effects of CO₂ build up in the atmosphere. If successful, it is claimed that CO₂ output could
35 be reduced by as much as 90 %.³ The captured CO₂ could then be recycled into other avenues
36 such as enhanced oil recovery or chemical feedstock production.

37

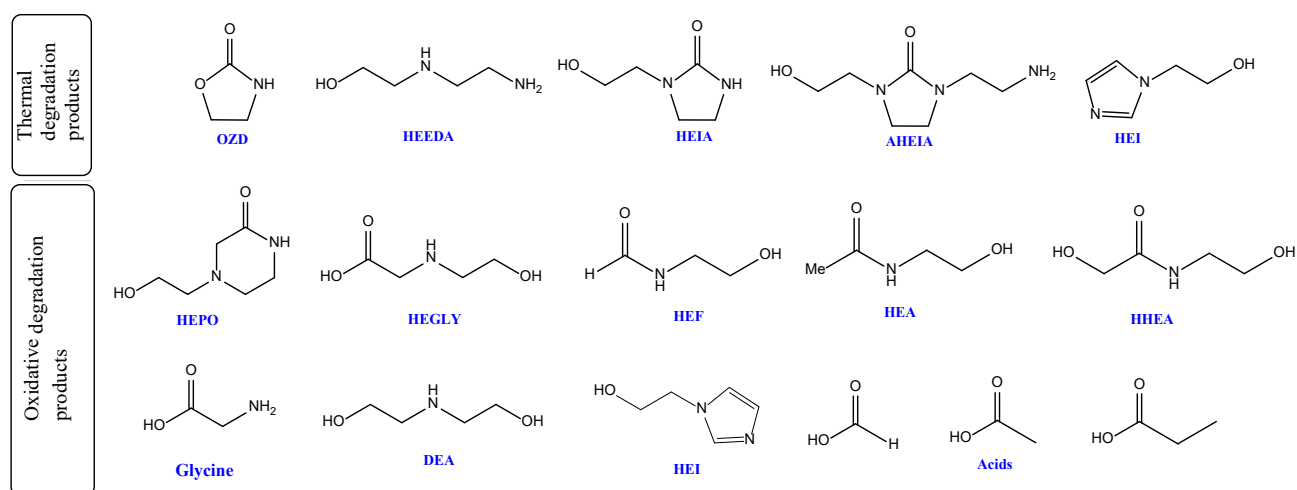
38 A number of different technologies have been investigated for capturing CO₂ post combustion,
39 all with varying levels of success. For example, absorption of the gas has been attempted using
40 metal organic frameworks.⁴⁻⁷ To date however, one of the most successful and commercially
41 advanced technologies employs the use of amine based solvents. It has been successfully
42 adopted in The Boundray Dam Integrated Carbon Capture and Storage Project in Canada.⁸ The
43 plant has the ability to capture over 1 million tonnes of CO₂ each year and is currently the
44 largest commercial scale facility of its kind.

45

46 The accepted industrial standard amine for carbon capture is monoethanolamine (MEA).⁹
47 However, further amines such as 2-amino-2-methyl-1-propanol (AMP), diethanolamine (DEA)
48 ,^{10, 11} ethylenediamine (EDA),¹²⁻¹⁴ methyldiethanolamine (MDEA)¹⁵ all have similar CO₂
49 absorption rates to MEA and have been studied.¹⁶ Regardless of the choice of amine, there are
50 a number of requisite features to be commercially viable. It should have good solubility and
51 must react rapidly and reversibly with CO₂. Current systems are hindered by the cost of solvent
52 regeneration which has been reported to be as high as 10 % of the total costs involved in the
53 process and degradation of the amine.¹⁷

54

55 Degradation of the amine can occur thermally or oxidatively. Thermal degradation has been
 56 extensively studied over a long period of time by many research groups.^{9, 18} It occurs mainly
 57 in the stripper at temperatures between 100 and 120 °C and generally increases with increased
 58 CO₂ loading. The principle products of MEA degradation have been identified as 2-
 59 oxazolidinone (OZD), N-(2-hydroxyethyl)ethylenediamine (HEEDA), N-(2-aminoethyl)-N'-
 60 (2-hydroxyethyl)imidazolidin-2-one (AHEIA), 1-(2-hydroxyethyl)imidazolidone (HEIA),
 61 and N-(2-hydroxyethyl)imidazole (HEI) as shown in **Figure 1**. Mechanisms to rationalize their
 62 formation have been reported by kim and Sartori¹⁹ and later built upon by Davis et al.²⁰ It is
 63 generally accepted that the process begins with cyclisation of the carbamate species to form
 64 OZD. This species can then undergo a ring opening reaction with a second molecule of MEA
 65 to form HEEDA. HEIA or AHEIA can subsequently be formed from HEEDA.



66

67 **Figure 1:** Major thermal and selected oxidative degeneration products of MEA

68

69 Oxidative degeneration is less well understood compared to thermal degradation. However it
 70 has received more attention over the last two decades as oxidative degradation products are by
 71 far the most observed species under real plant conditions.²¹⁻²³ The process occurs mainly in
 72 the absorber in the presence of oxygen. It is considered to be radical driven, with an electron
 73 loss from the amine nitrogen or hydrogen loss from the carbon atom α or β to the nitrogen
 74 initiating the degradation.^{21, 24-27} Which of these mechanisms dominates is dependent on the
 75 pH of the system, the nature of the oxidant, the concentration and nature of the amine species.
 76 ^{21, 24-27} The degradation products are normally split into two classes: primary and secondary.
 77 Primary species are formed directly from the amine. They include, but are not limited to,

78 ammonia, methylamine, aldehydes and carboxylic acids. Secondary degradation products are
79 formed from primary products and include, for example, N-(2-hydroxyethyl)acetamide (HEA),
80 2-hydroxy-N-(2-hydroxyethyl)acetamide (HHEA), N,N'-bis(2-hydroxyethyl)oxalamide
81 (BHEOX), N-(2-hydroxyethyl)glycine (HEGly) and 1-(2-hydroxyethyl)piperazine-2-one
82 (HEPO) (**Figure 1**). The number of observed products in laboratory degradation experiments
83 is vast. Five different research teams have reported as many as 60 different species.²⁸⁻³² The
84 formation of many of these species is still unclear. Evidently, an understanding of the
85 mechanistic steps leading to the formation of all of these species would, whilst challenging, be
86 of considerable use in optimizing the performance of amine-based systems. With the vast
87 number of observed products from degradation, molecular modelling can be of significant use
88 in analyzing the formation of these species.

89

90 Despite this, the number of computational studies directly focused on the degradation steps in
91 these systems remains limited. Vevelsted et al modelled the formation of multiple degradation
92 products from MEA using static quantum mechanical (QM) calculations and reported most to
93 form favorably.³³ Saeed and coworkers looked into the mechanism of formation of
94 imidazolidinone from MEA.³⁴ More recently Yoon et al reported first principle studies on both
95 the thermal degradation of MEA and EDA.^{35,36} Xie et al investigated the different mechanisms
96 of both AMP and MEA reacting with CO₂.³⁷ To date, there have been few detailed modelling
97 studies conducted into wider product formation with most studies focusing on a small subset
98 of reactions.

99

100 In the current paper, we use DFT to investigate the formation of many degradation species.
101 Mechanisms are postulated and subsequently modelled to rationalise the formation of
102 formaldehyde, formic acid, methylamine, MAE, glycine, glycolic acid, HEI, DEA, DMA,
103 HEGly, ethanoic acid and ethanal.

104

105

106

107 2. Computational details

108 All calculations were performed on Gaussian 09, revision D.01.³⁸ The B3LYP functional³⁹⁻⁴¹
109 and cc-PVTZ⁴² basis set were used throughout this study with the ultrafine setting for the
110 integrals. This setup was chosen to be consistent with previously published work within the
111 group and to allow for comparisons with that work.⁴³ Benchmarking studies also show that
112 this setup can provide reasonable results within an acceptable time frame.^{44, 45} Solvent effects
113 were accounted for using the default Polarizable Continuum Model (PCM) as implemented in
114 Gaussian 09.⁴⁶ The solvent parameters for water were used in each case.⁴⁷ Selected
115 calculations were carried out using the SMD solvent method and can be found in the supporting
116 information. Calculations are reported at 298.15 K. Empirical dispersion corrections through
117 the GD3 keyword were applied to all calculations.⁴⁸ Optimized structures were confirmed as
118 stationary points by the absence of imaginary frequencies. Transition states were confirmed
119 both by the presence of one large negative frequency corresponding to the expected saddle
120 point and with intrinsic reaction coordinate scans (IRCs). Transition states were optimized
121 using the QST3 method as implemented in Gaussian.⁴⁹ Free energies were improved using the
122 Grimme quasiharmonic entropy correction using the GoodVibes script.⁵⁰ A further set of
123 calculations for all reactions modelled here using the m06 functional⁵¹ and def2TVP basis set
124 is provided in the supporting information

125

126 3. Results and Discussion

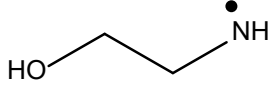
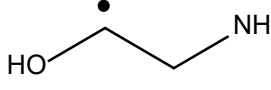
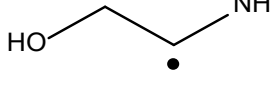
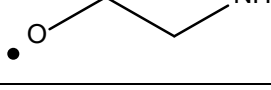
127 3.1 Formation of MEA radicals and subsequent fragmentation

128

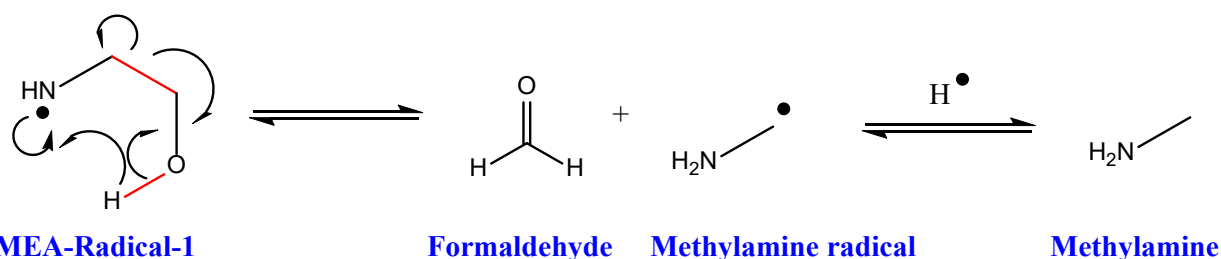
129 Our first consideration was to the formation of the amine radical from MEA. There are four
130 proton sites on MEA where abstraction could occur: at the nitrogen (-NH), either carbon (-
131 CH₂) or the oxygen (-OH). For each potential site, the proton abstraction was modelled with
132 each of three different radicals: Ethyl●, HO● and O₂. The activation energies for all these
133 reactions are given in **Table 1**. The lowest observed activation energies involved reactions of
134 MEA with a hydroxyl radical (HO●) followed by an ethyl radical and finally oxygen. However,
135 all are surmountable given standard experimental conditions.

136

137 **Table 1:** Activation energies for the formation of four different radicals from MEA after
 138 reaction with three different radicals.

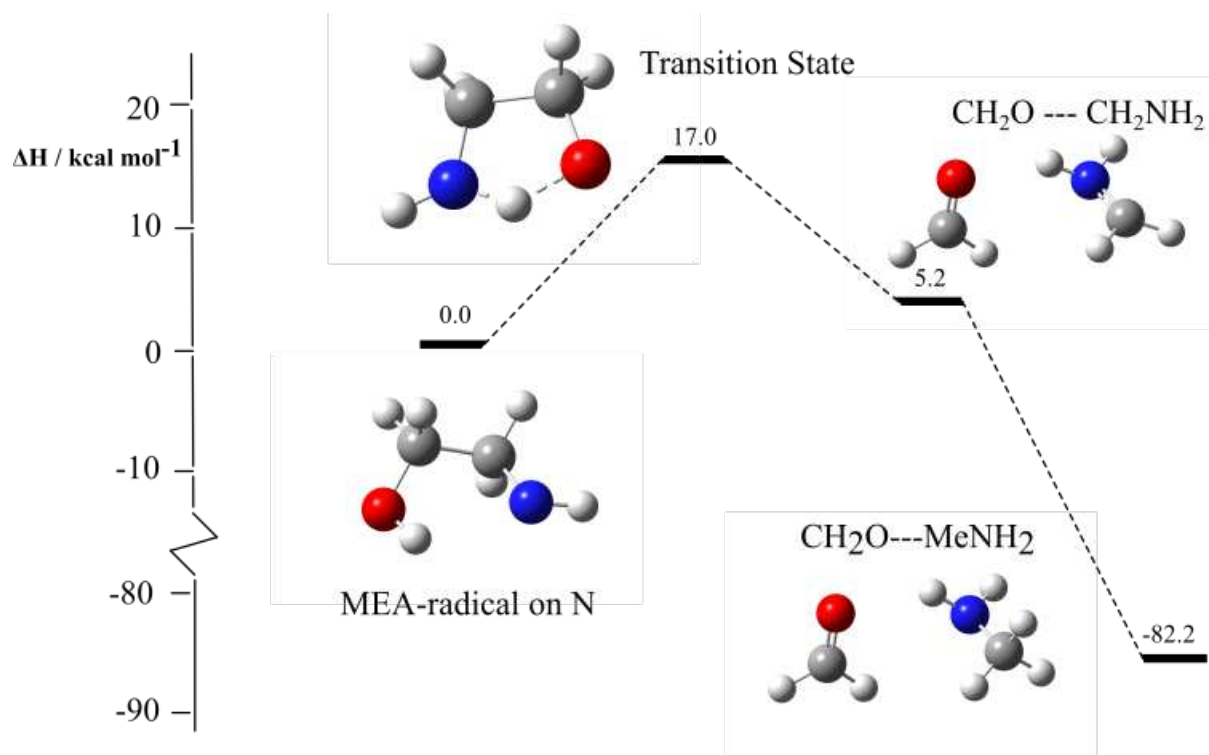
MEA radical formed	Label	Activation energy for radical reaction / kcal mol ⁻¹		
		Ethyl	OH	O ₂
	MEA-Radical-1	10.7	2.3	31.7
	MEA-Radical-2	11.0	3.1	32.0
	MEA-Radical-3	9.6	2.2	26.5
	MEA-Radical-4	8.4	4.4	32.2

139
 140 Regardless of the origin of the MEA radical species, there are a number of ways each one can
 141 break down to form primary degradation products. Here, we consider each in turn. **Scheme**
 142 **1** shows a plausible mechanism for fragmentation from the nitrogen-localized radical species
 143 (**MEA-Radical-1**). This mechanism was first presented by Patryaev et al. and could lead to
 144 the formation of formaldehyde and methylamine.⁵²



146 **Scheme 1:** Suggested formation of formaldehyde and methylamine from a **MEA-Radical-1**.
 147 (Bonds broken during the reaction shown in red)

148
 149 In this fragmentation, the MEA radical undergoes an intramolecular rearrangement where the
 150 OH bond is broken as is the carbon-carbon bond (shown in red in **Scheme 1**). This coincides
 151 with the formation of an N-H bond. The DFT-calculated energy profile is shown in **Figure 2**.



152

153 **Figure 2:** DFT-calculated ΔH energy profile for the proposed formation of formaldehyde and
 154 methylamine from a **MEA-Radical-1**.

155

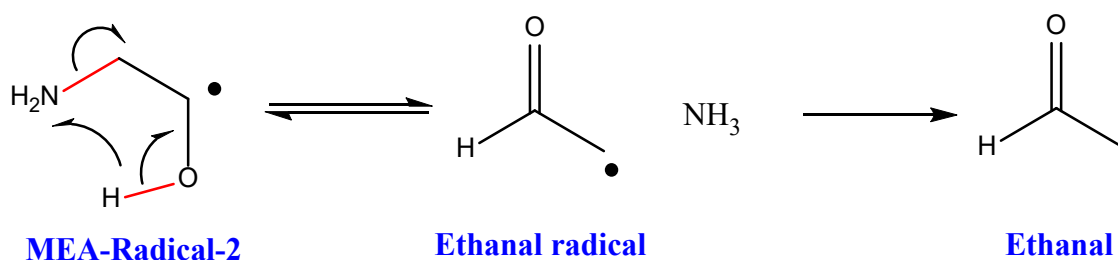
156 The activation energy for this reaction is only $17.0 \text{ kcal mol}^{-1}$, which is easily surmountable
 157 given the experimental conditions. The initial fragmentation leads to the formation of a
 158 methylamine radical species, which can form methylamine given a further hydrogen radical
 159 source. This radical recombination step is clearly very favorable.

160

161 Abstraction of a hydrogen radical from the β carbon to the nitrogen leads to a species that can
 162 fragment to form acetaldehyde and ammonia as shown in **Scheme 2 (MEA-Radical-2)**.

163

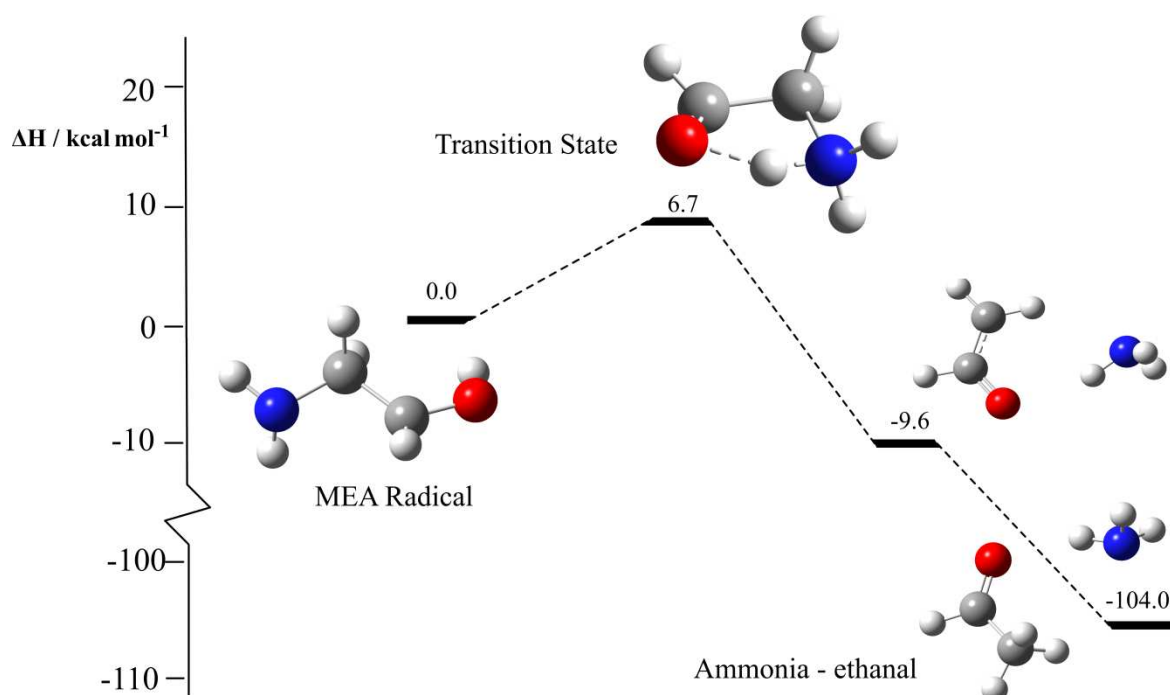
164



165

166 **Scheme 2:** Suggested formation of acetaldehyde and ammonia from a **MEA-Radical-2**.

167 (Bonds broken during the reaction shown in red)

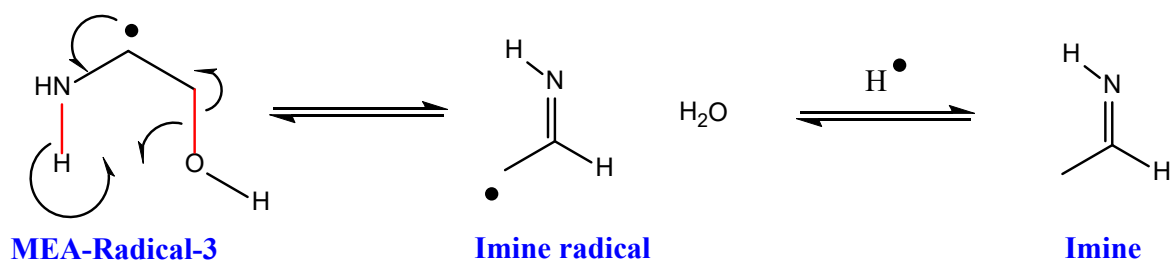


168

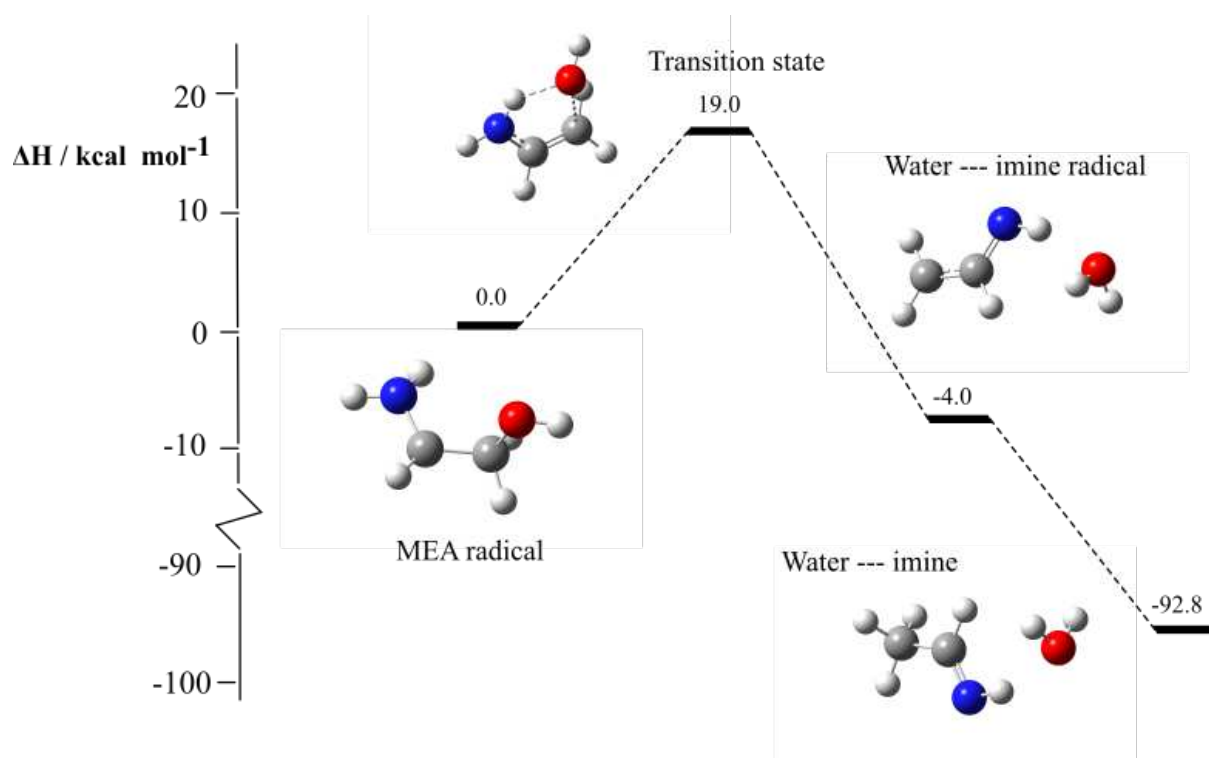
169 **Figure 3:** DFT-calculated ΔH energy profile for the proposed formation of ammonia and
 170 ethanal from **MEA-Radical-2**.

171

172 Here, the OH bond is broken, alongside the breaking and forming of N-H bonds. The energy
 173 profile in **Figure 3** is similar to that in **Figure 2**. The activation energy for this reaction is very
 174 low (+6.7 kcal mol⁻¹) and radical recombination is very favorable. The ethanal formed from
 175 fragmentation of this radical can be further oxidized in the presence of oxygen to form ethanoic
 176 acid. Organic acids have implications elsewhere where they can react with MEA to form amide
 177 species.



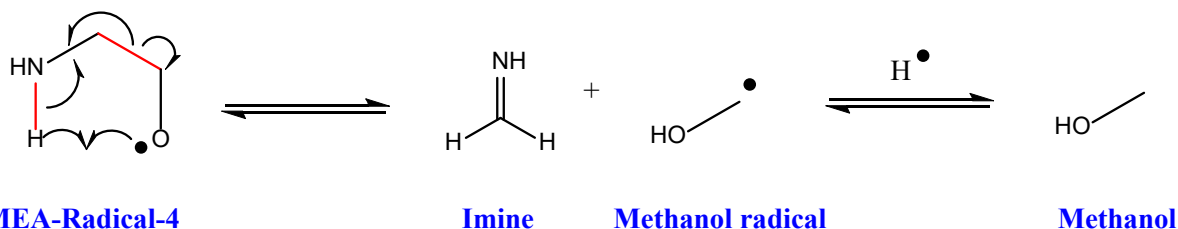
179 **Scheme 3:** Suggested formation of an imine and water from a **MEA-Radical-3**. (Bonds
180 broken during the reaction shown in red)



185 The third fragmentation reaction involves breakdown from a radical localized on the $C\alpha$ to the
186 nitrogen (**MEA-Radical-3**). Breaking of NH and OH bonds concurrently with formation of a
187 further OH bond leads to water and an imine species. **Figure 4** shows this reaction has the
188 highest activation energy of all the fragmentations thus far but is still surmountable under the
189 typical experimental conditions.

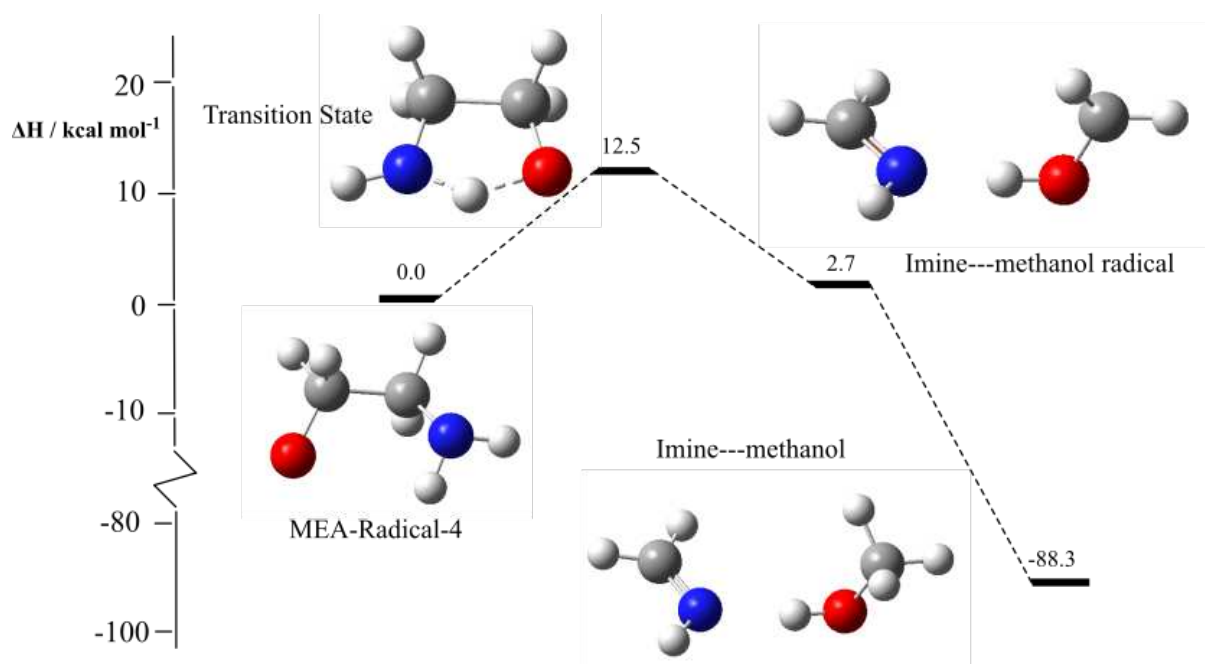
190

191 The final fragmentation reaction involves the formation of an imine and methanol from **MEA-Radical-4**,
 192 **Radical-4**, as shown in **Scheme 4**. Here, concurrent breaking of an N-H and the C-C bonds
 193 and formation of a new OH bond yields the target species. As shown in **Figure 5**, this reaction
 194 is predicted to have a low activation energy of 12.5 kcal mol⁻¹ and again radical recombination
 195 can help to drive the reaction forward.



197 **Scheme 4:** Suggested formation of methanol and an imine from a **MEA-Radical-4**. (Bonds
 198 broken during the reaction shown in red)

199



201 **Figure 5:** DFT-calculated ΔH energy profile for the proposed formation of an imine and
 202 methanol from a **MEA-Radical-4**.

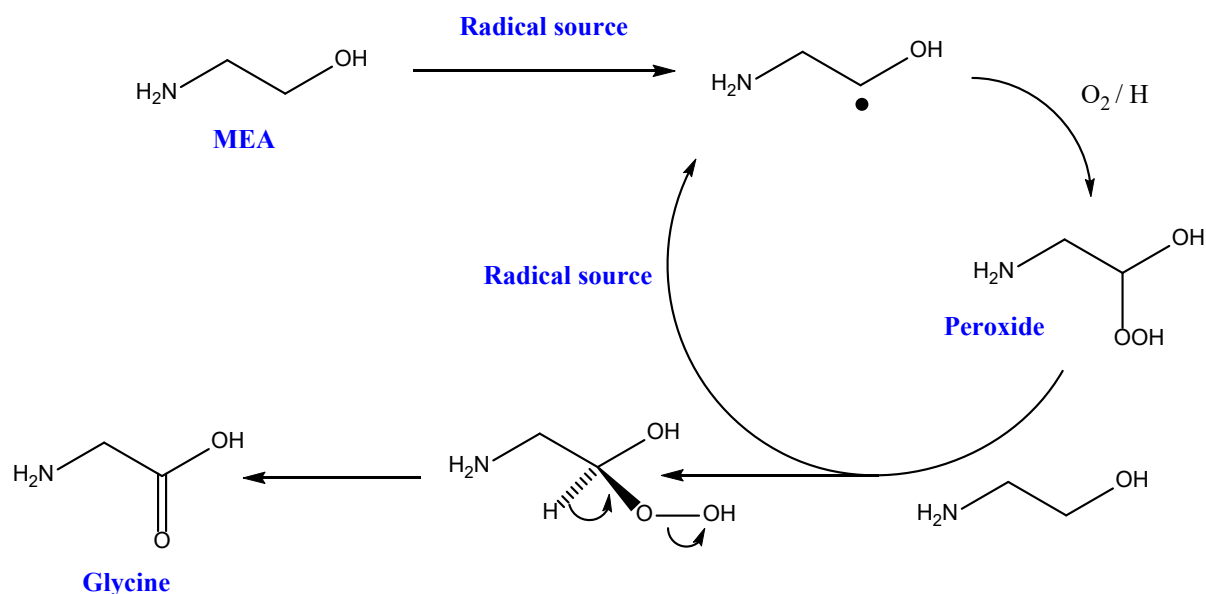
203

204 Overall, data presented in **Figures 2-5** shows that fragmentation of the MEA radicals can lead
 205 to the formation of water, ammonia, formaldehyde, methylamine, methanol and various imines
 206 dependent on the location of the initial MEA radical.

207 **3.2 Glycine and HEGly formation**

208

209 If the concentration of oxygen in the system is sufficiently high, rapid radical recombination
210 can occur to form a peroxide species. Bedell proposed that the peroxide species can then break
211 down to form glycine as shown in **Scheme 5**.^{53, 54}

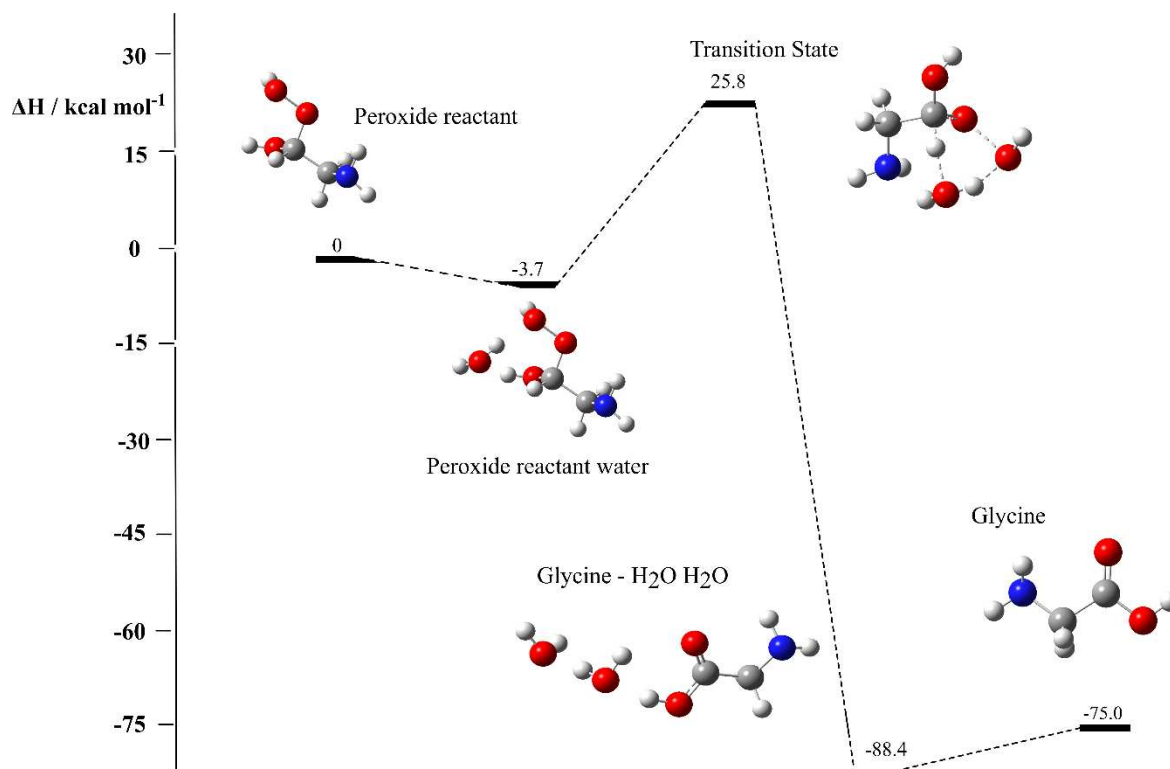


212

213 **Scheme5:** Suggested formation of glycine from MEA

214 We recently reported on the formation of the peroxide species, which had an activation energy
215 of 28.7 kcal mol⁻¹.⁴³ Upon its formation, two different degradation paths are possible: one
216 which eliminates HOOH and a further deprotonation reaction which can lead to the formation
217 of glycine. **Figure 6** shows that formation of glycine, through elimination of water is
218 surmountable. The activation energy for HOOH elimination is 28.5 kcal mol⁻¹ compared to
219 29.5 kcal mol⁻¹ for glycine formation. Whilst there is a marginal preference for elimination of
220 HOOH, it is likely that both species can be observed.

221



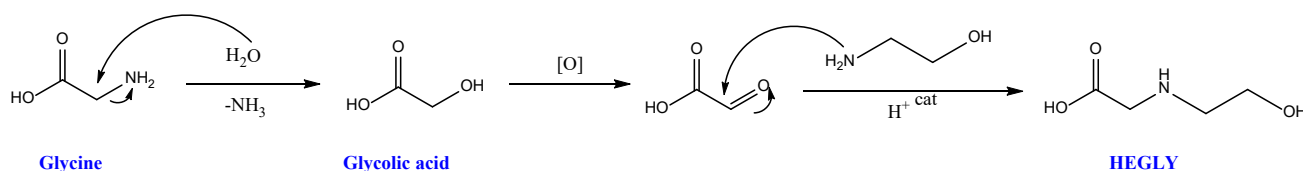
222

223 **Figure 6:** DFT-calculated ΔH energy profile for the formation of glycine from a peroxide
 224 species.

225

226 The glycine generated here can undergo further reactions to form glycolic acid. If the hydroxyl
 227 group (-OH) were to oxidize to form an aldehyde, this would generate a precursor to the
 228 formation of HEGly. The process is summarized in **Scheme 6**.

229



230

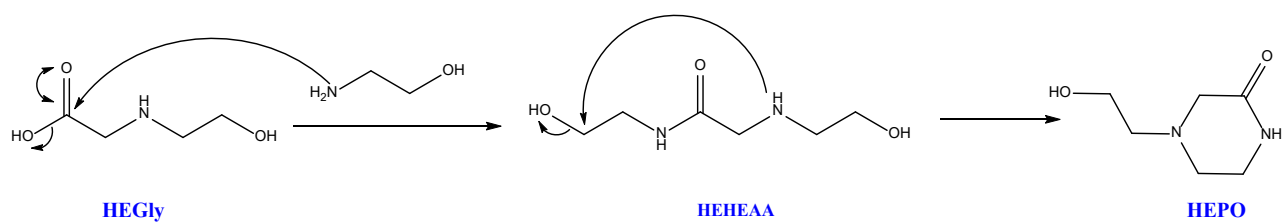
231 **Scheme 6:** Proposed route to the formation of HEGly from glycine

232

233 **Figure 7** shows the formation of HEGly from MEA. Initially, the nitrogen atom on MEA acts
 234 as a nucleophile and binds to the carbonyl carbon atom of the acid reactant. The activation
 235 energy for the first hydrogen transfer reaction is $26.3 \text{ kcal mol}^{-1}$ and can likely be further

236 reduced by transfer to and from an explicit water molecule as we have shown elsewhere.⁴³ A
237 second hydrogen transfer reaction eliminates water and forms an imine species. This imine
238 species can pick up a proton from any source, most likely MEAH⁺. This reaction eliminates
239 CO₂. Finally, the anionic product can pick up a proton to form HEGly. HEGly is a precursor
240 to HEHEAA, which in turn can cyclise to form HEPO. **Scheme 7** summarises this process.

241



Scheme 7: Potential route to the formation of HEPO from HEGly

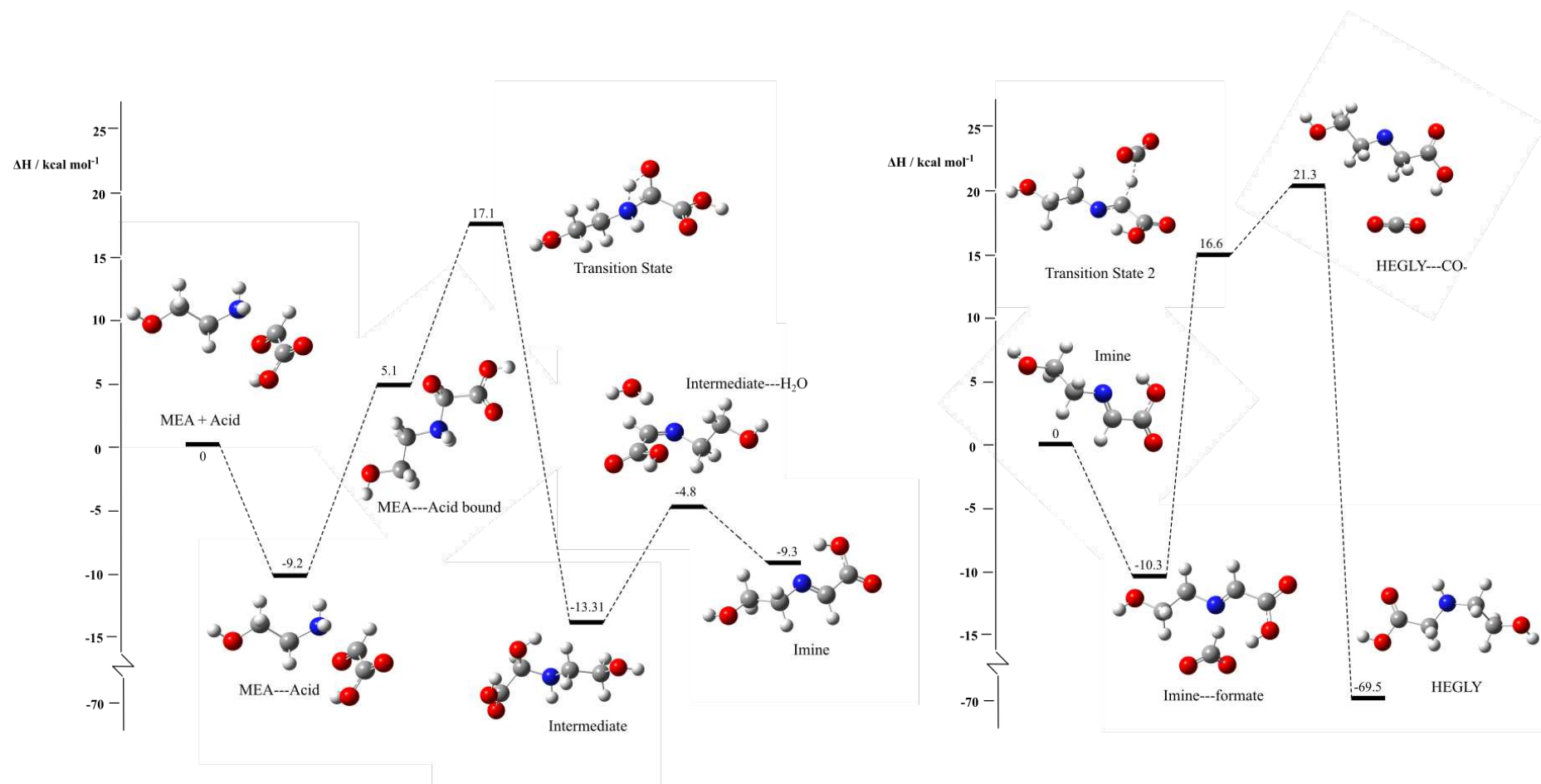
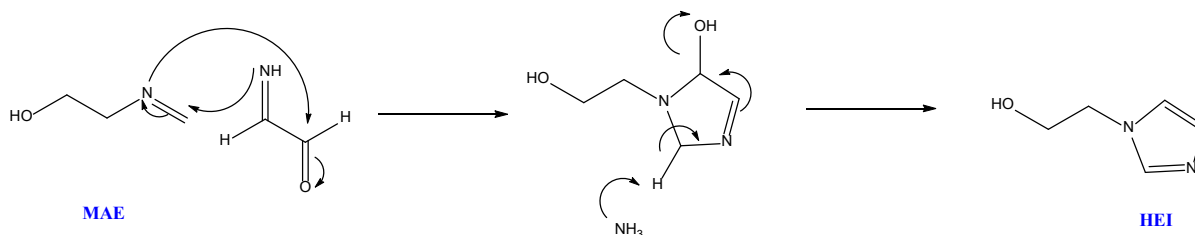


Figure 7: DFT-calculated ΔH energy profiles for the formation of an imine (left) and HEGLY from the imine (right)

247 **3.3 HEI formation**

248

249 HEI is a major degradation product observed in pilot plants. A mechanism to explain its
 250 formation was proposed by Vevelstad,⁵⁵ which itself was an adaptation from a patent by
 251 Katsuura and Washio.⁵⁶ **Scheme 8** shows how two imine species react to form an intermediate
 252 species, which can subsequently form HEI after several proton transfers.

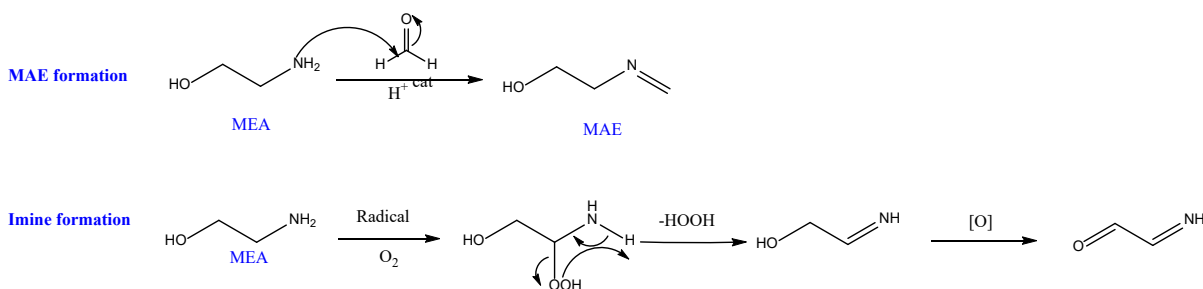


253

254 **Scheme 8:** Suggested formation of HEI from two imine species.

255

256 For this route to be viable, the origin of the reactants must also be rationalized. MAE can
 257 potentially be formed *via* the reaction of MEA and formaldehyde. As formaldehyde can be
 258 formed from the fragmentation reactions of MEA radicals, as postulated in **Section 3.2**, the
 259 constituent parts are all present to form MAE. The second imine, can be formed from oxidation
 260 of an amino alcohol, which itself is formed during the fragmentation of MEA radicals. Both
 261 processes are summarized in **Scheme 9**.



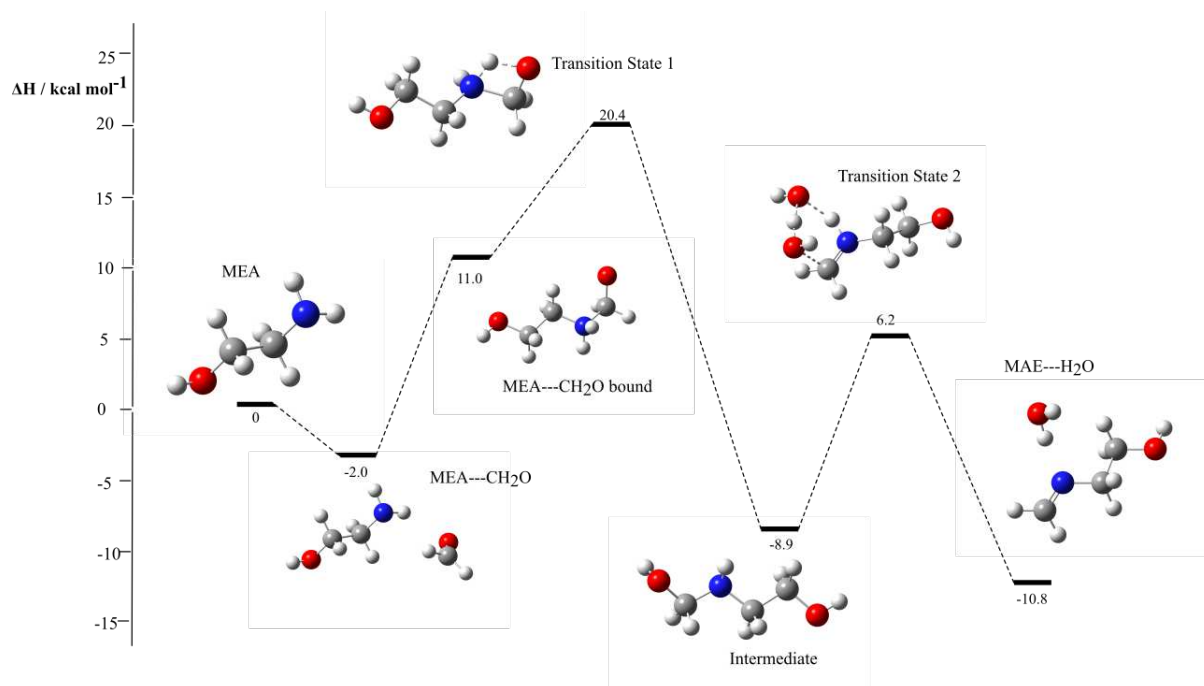
262

263 **Scheme 9:** Suggested routes to imine formation from MEA.

264

265 The DFT-calculated energy profile for the formation of MAE is shown in **Figure 8**. The
 266 reaction is initiated by nucleophilic attack of MEA on the formaldehyde. Two successive

267 proton transfers yield MAE and water. The first activation energy is 22.4 kcal mol⁻¹, and the
268 second is 15.1 kcal mol⁻¹, which are surmountable under the experimental conditions.



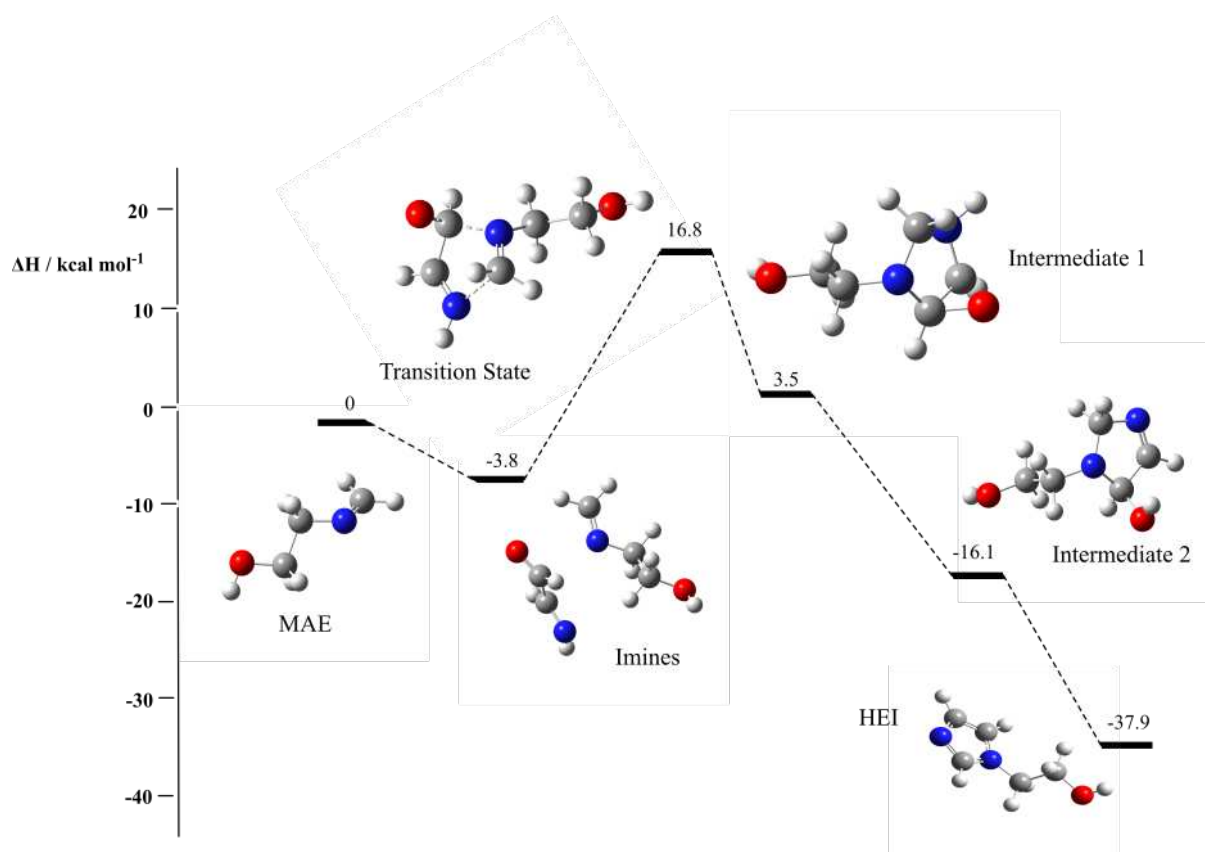
269

270 **Figure 8:** DFT-calculated ΔH energy profile for the proposed formation of MAE from MEA
271 and formaldehyde.

272

273 The formation of HEI is presented in **Figure 9**. The two imines in close proximity are 3.8 kcal
274 mol⁻¹ more stable than when infinitely separated. The activation energy is 20.6 kcal mol⁻¹.
275 After cyclisation, the intermediate species undergoes successive proton transfers, most likely
276 assisted by water or further molecules of MEA, which help to facilitate movement of the

277 protons. The product, HEI, is $37.9 \text{ kcal mol}^{-1}$ more stable than the separated reactants.

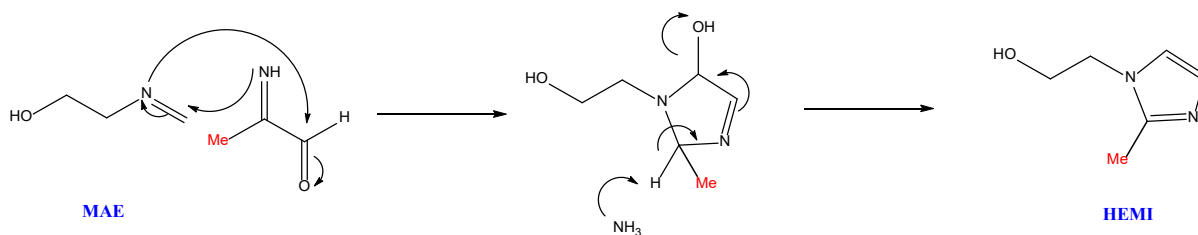


278

279 **Figure 9:** DFT-calculated ΔH energy profile for the formation of HEI from two imine
280 species.

281

282 Whilst no calculations were undertaken here, it is noted that this route to HEI formation could
283 be modified to form substituted variants of HEI as shown in **Scheme 10**. For example,
284 Vevelstad proposed the formation of N-(2-hydroxyethyl)-2-methylimidazole (HEMI) where a
285 proton on the five membered ring is replaced with a methyl substituent.⁵⁵ If the appropriate
286 imine was suitably substituted, then this would lead to the formation of HEMI. (The substituent
287 change is highlighted in red in **Scheme 10**)



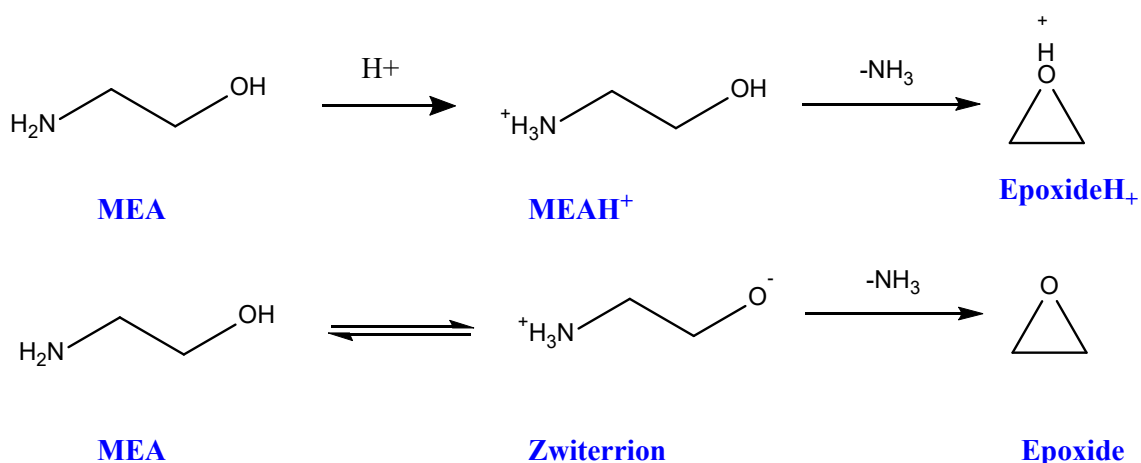
288

289 **Scheme 10:** Suggested formation of HEMI from two imine species.

290 **3.4 Epoxide formation**

291

292 The degradation of MEA into ammonia and an epoxide has been suggested by Lepaumier.²⁷
 293 The reaction is shown in **Scheme 11**. Prior protonation of the nitrogen on MEA acts to create
 294 a more labile leaving group and thus can drive the reaction. Given that the formation of acids
 295 is possible originating from the fragmentation of MEA radicals, this is possible under the
 296 experimental conditions. A further route to the formation of epoxides would be from a
 297 zwitterionic form of MEA, ($\text{H}_3\text{N}^+\text{CH}_2\text{CH}_2\text{O}^-$). The anionic oxygen can attack the carbon alpha
 298 to the nitrogen, which eliminates ammonia.

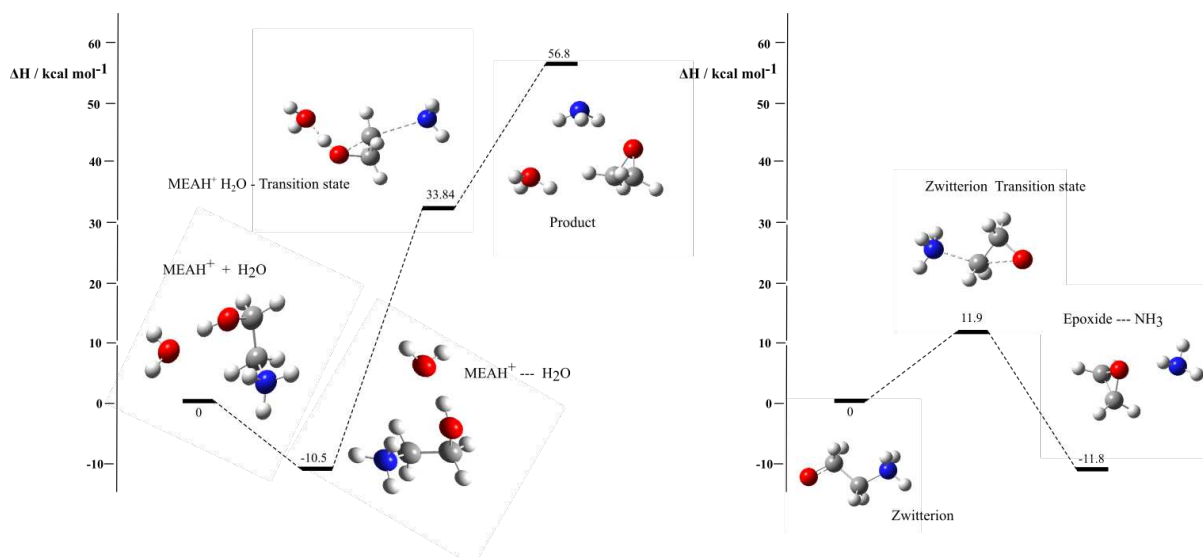


299

300 **Scheme 11:** Potential route to the formation of epoxides and ammonia from MEA.

301

302 **Figure 10** shows that the energy profiles for both pathways. The activation energy for the
 303 reaction of protonated MEA is appreciably high ($44.3 \text{ kcal mol}^{-1}$). Moreover, the reaction is
 304 highly endothermic. Given that the product is a highly strained three-membered ring, this
 305 observation is expected. This route is not responsible for the formation of epoxides. The
 306 reaction from the zwitterion has a much lower activation energy of $11.9 \text{ kcal mol}^{-1}$ and the
 307 overall reaction is exothermic. This suggests that there is a potential route to the formation of
 308 epoxides in the experimental media. However, a consideration must be given to the origin of
 309 the zwitterion, which is $31.8 \text{ kcal mol}^{-1}$ higher in energy than MEA. As this is a charged
 310 species, the product can likely be stabilized significantly by interaction with water molecules
 311 and thus this route is potentially viable overall.

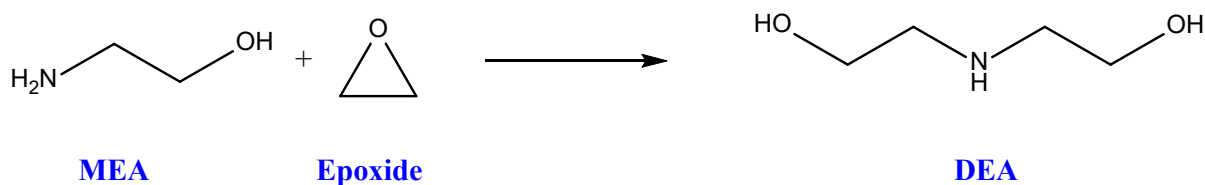


312

313 **Figure 10:** DFT-calculated ΔH energy profile showing two potential routes to the formation
 314 of epoxides from MEA (left) and from a zwitterion (right).

315

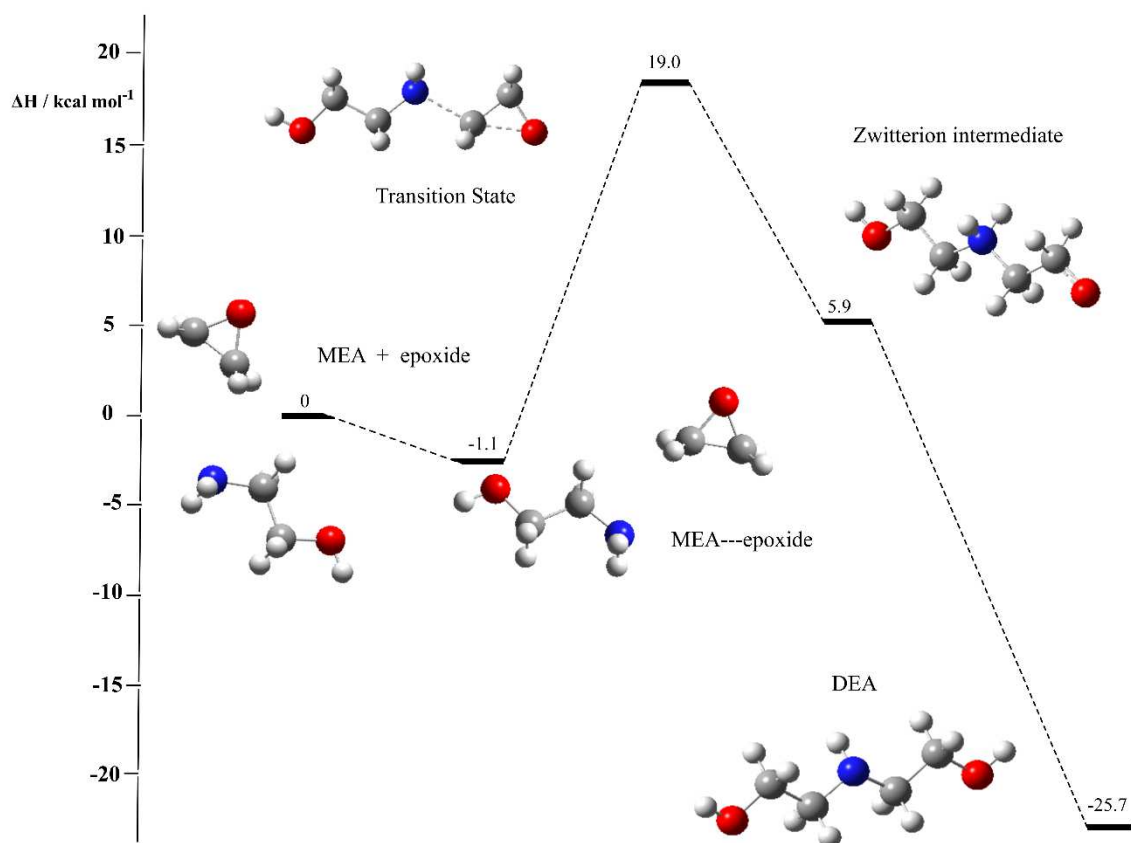
316 Whilst a thorough investigation into all the amine species which could react in this manner is
 317 beyond the scope of this work, we present the reaction with MEA as an illustration. **Scheme**
 318 **12** shows the formation of DEA from MEA and a protonated epoxide.



319

320 **Scheme 12:** Potential route to the formation of DEA from MEA and an epoxide.

321



322

323 **Figure 11:** DFT-calculated ΔH energy profile for the formation of DEA from MEA and
 324 epoxide.

325

326 **Figure 11** shows the energy profile for the proposed formation of DEA from MEA and an
 327 epoxide. Initially, the nitrogen atom of MEA acts as a nucleophile and reacts with one of the
 328 carbon centers on the epoxide. This effects a ring opening and forms a zwitterion which can
 329 rapidly rearrange to form DEA. The activation energy for the reaction is $20.1 \text{ kcal mol}^{-1}$ and
 330 the reaction is highly exothermic overall.

331

332

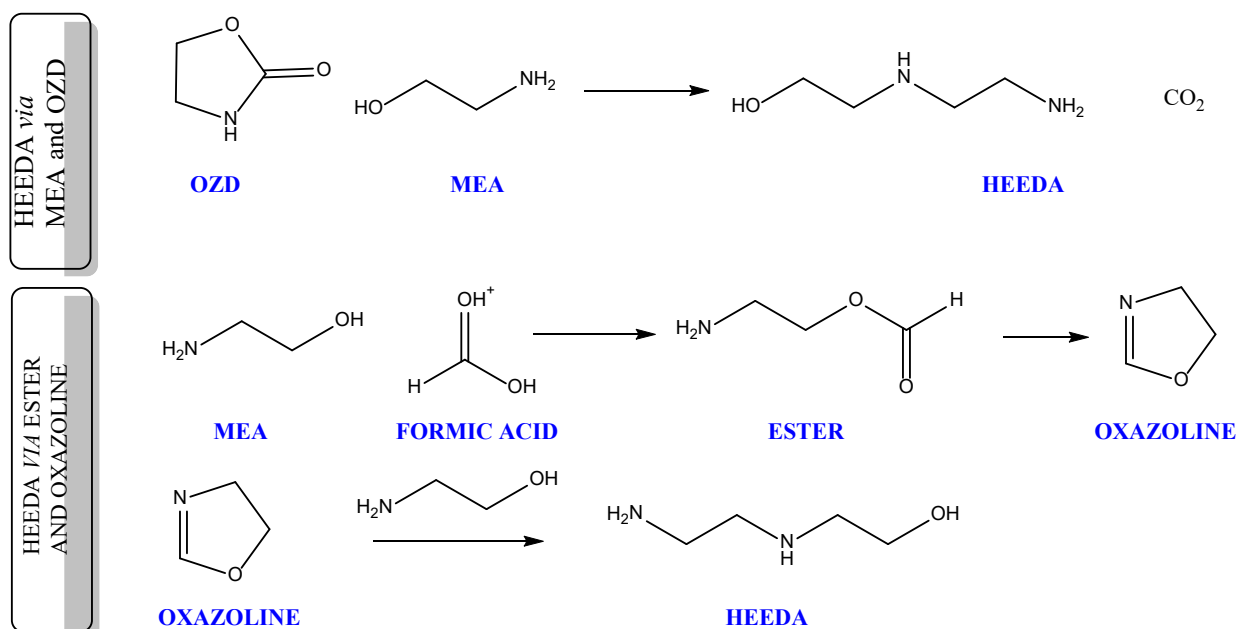
333

334 **3.5 HEEDA and BHEEDA**

335

336 We recently reported on the formation of HEEDA *via* the ring opening reaction of OZD and
 337 MEA.⁴³ This reaction was calculated to have an activation energy of 27.3 kcal mol⁻¹. Here,
 338 we present an alternative pathway to the formation of HEEDA *via* an oxazoline intermediate.
 339 Both routes are shown in **Scheme 13**. In the second route, MEA undergoes an acid-catalysed
 340 esterification reaction with formic acid to initially form an ester. The ester can potentially
 341 cyclise to form an oxazoline, which can subsequently undergo a ring opening reaction with
 342 MEA to form HEEDA.

343

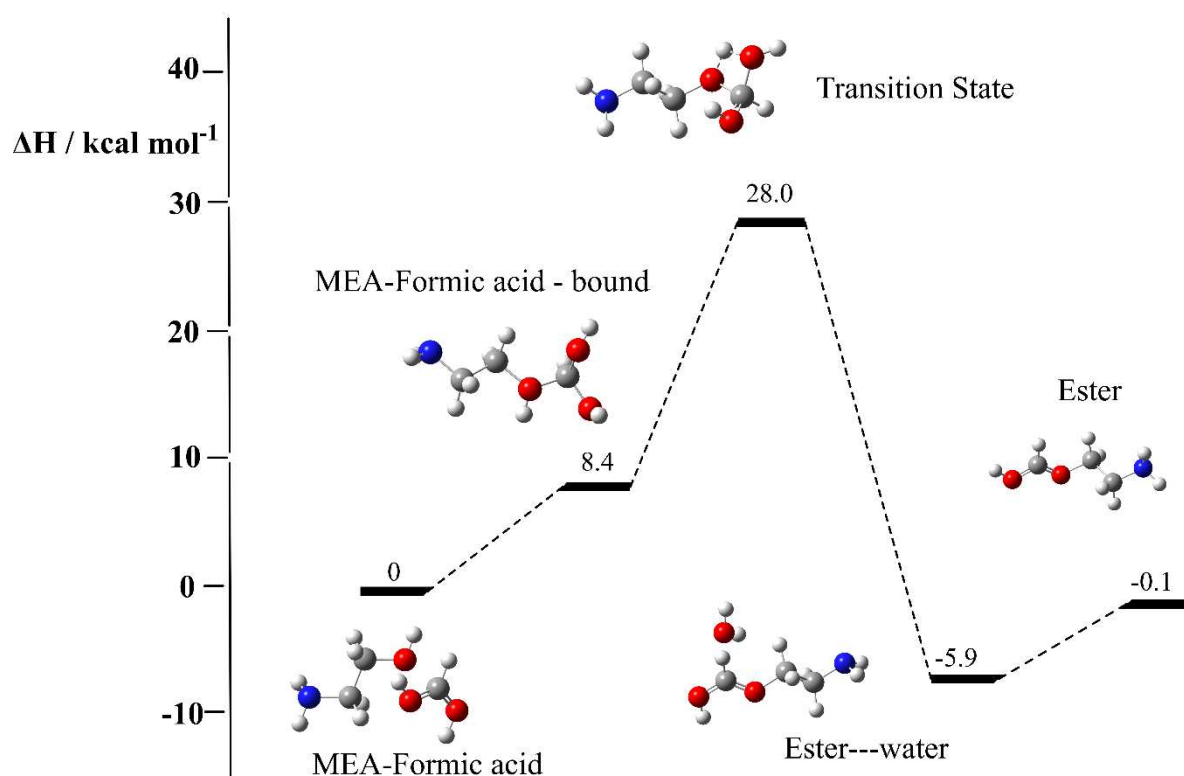


344

345 **Scheme 13:** Two routes to explain the formation of HEEDA. Above: From OZD and MEA.

346

Below: From MEA and formic acid.

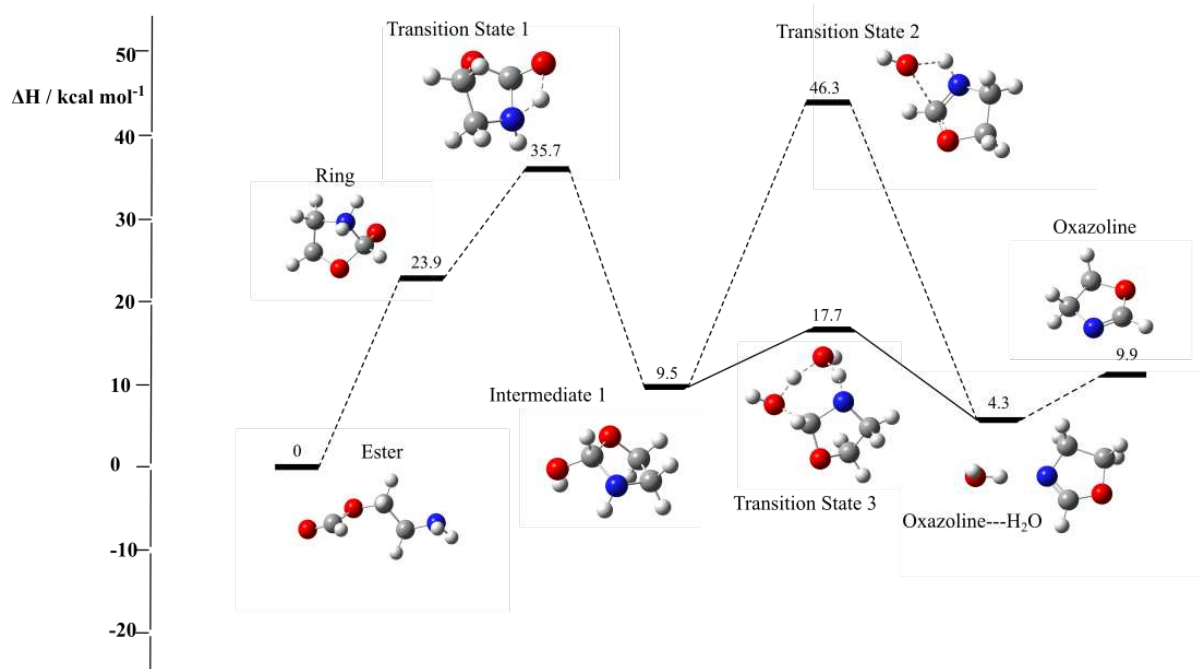


347

348

349 **Figure 12:** DFT-calculated ΔH energy profile for the formation of an ester from MEA and
 350 formic acid.

351 The energy profile for the initial formation of the ester is shown in **Figure 12**. The ester is
 352 formed from a nucleophilic attack of the MEA oxygen on the carbonyl carbon of formic acid.
 353 Hydrogen transfer from the MEA hydroxyl (-OH) group to an OH group on the carbonyl allows
 354 for the elimination of water and formation of the target product. This reaction will be
 355 competitive with the formation of an amide, again from the same reactants. We reported on the
 356 formation of the amide species previously, HEF, from these reactants which had an activation
 357 energy of $40.1 \text{ kcal mol}^{-1}$.⁴³ The activation energy reported here for ester formation is lower
 358 and would therefore be favoured.



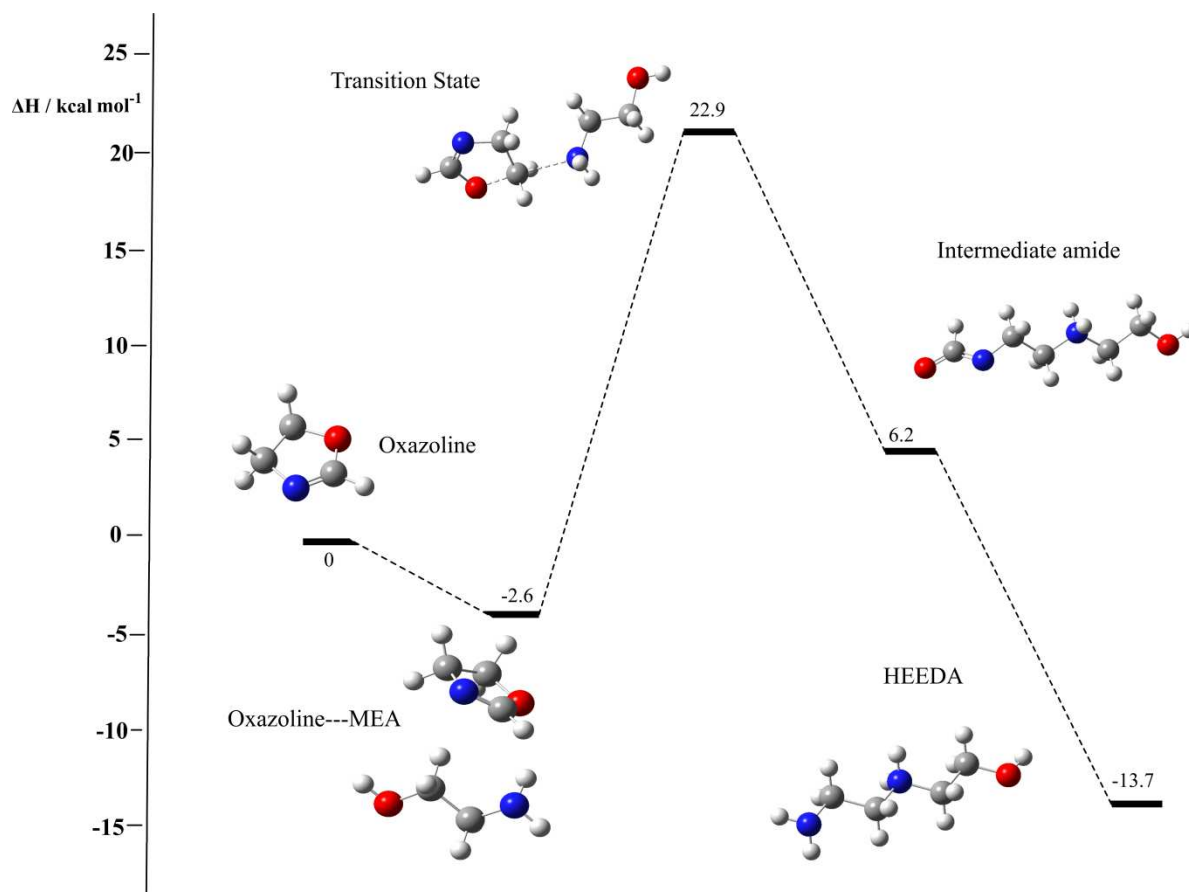
360

361 **Figure 13:** DFT-calculated ΔH energy profile for the formation of oxazoline from as ester.

362

363 We next turned our attention to the formation of oxazoline from the ester. **Figure 13** shows
 364 the energy profile for this reaction. The reaction is initiated by nucleophilic attack of the ester
 365 nitrogen on the carbonyl carbon. Two successive proton transfers from the nitrogen to the
 366 pendant oxygen allows for the elimination of water and the formation of oxazoline. The second
 367 proton transfer reaction has a high activation energy of 46.3 kcal mol^{-1} (**Transition State 2**),
 368 although this barrier can be significantly lowered by hydrogen transfer to and from explicitly
 369 included water molecules (**Transition State 3**). In this case, the activation energy is 17.7 kcal
 370 mol^{-1} .

371



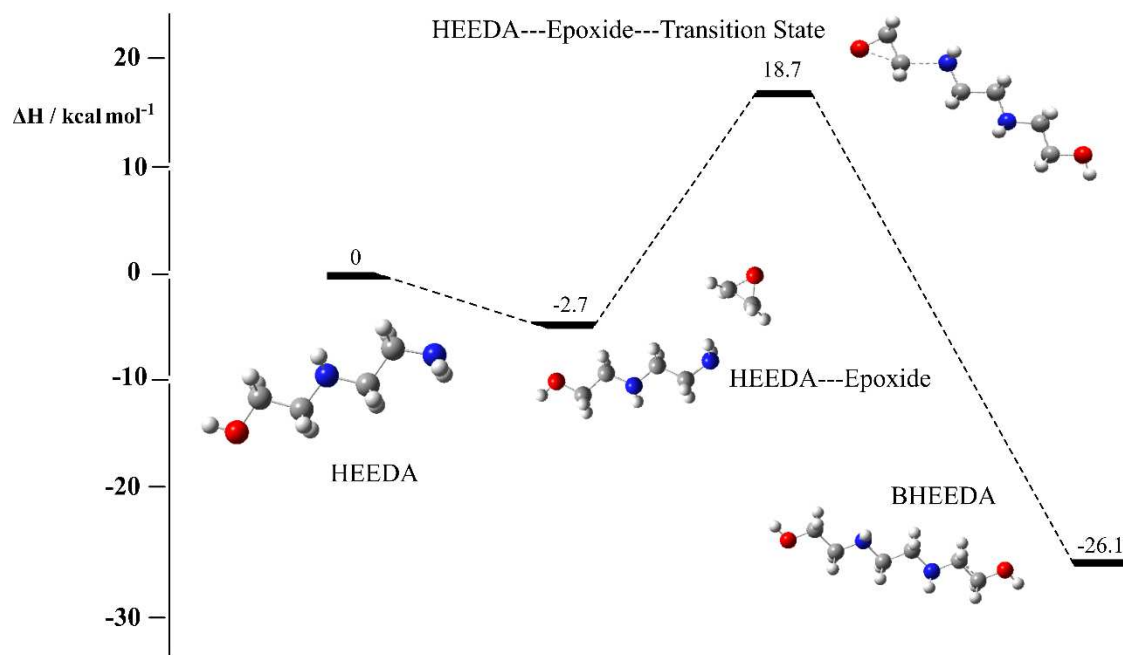
372

373 **Figure 14:** DFT-calculated ΔH energy profile for the formation of HEEDA from oxazoline
 374 and MEA

375

376 **Figure 14** shows the successive reaction where the oxazoline can be converted into HEEDA.
 377 As we have shown elsewhere, the nitrogen atom of the MEA acts as a nucleophile and attacks
 378 the carbon atom on oxazoline immediately connected to the oxygen. This causes the ring to
 379 open and forms a zwitterion intermediate. Rapid hydrogen transfer from the now cationic
 380 nitrogen centre to the anionic oxygen yields HEEDA. The activation energy is surmountable,
 381 at 25.5 kcal mol^{-1} . Whilst HEEDA formed in this way requires a significantly higher number
 382 of molecules and conversions when compared to the first reaction presented in **Scheme 13**, it
 383 acts to show that there are many potential routes to product formation in a complicated reaction
 384 media.

385



386

387 **Figure 15:** DFT-calculated ΔH energy profile for the formation of BHEEDA from HEEDA
 388 and epoxide.

389

390 Our final consideration was to the formation of BHEEDA from the reaction of HEEDA and an
 391 epoxide. The energy profile shown in **Figure 15** illustrates that the reaction has a relatively
 392 low barrier, 21.4 kcal mol⁻¹, and could easily form in pilot plants given the presence of HEEDA
 393 and epoxides.

394

395

396

397

398

399

400 4 Conclusions

401

402 In the current work, we have reported on DFT calculations investigating the chemical pathways
403 leading to the formation of degradation products of MEA. Activation energies were calculated
404 and scrutinized with respect to the experimental conditions to deduce which pathways were
405 most likely to lead to product formation.

406

407 MEA radicals were found to form from MEA in reactions with O₂, alkyl radicals and OH. Any
408 of the generated radicals can fragment leading to the formation of formaldehyde, methylamine,
409 water, ethanal, imines and ammonia. Under standard experimental conditions ethanal and
410 formaldehyde can oxidize to ethanoic acid and formic acid respectively.

411

412 Rapid radical recombination with oxygen can lead to a species which can degrade to form
413 glycine. Glycine can then react to initially form glycolic acid before further reactions to form
414 HEGly. A viable mechanistic pathway has been modelled to explain the formation of both HEI
415 and a substituted variant, HEMI. This involves the cyclisation of two imine species.

416

417 An alternative route to the formation of HEEDA has been presented. Initially, MEA reacts
418 with formic acid to form an ester. The ester species can cyclise to form oxazoline.
419 Nucleophilic attack of MEA on oxazoline can form HEEDA.

420

421 The mechanistic routes modelled here give good insight into the product formation observed
422 during MEA degradation. If sufficient modelling studies such as those presented here are
423 completed, then a full chemical kinetic model could be constructed. Such a model would offer
424 possibilities to modify the chosen amine and then predict product formation from degradation.
425 The work undertaken here would benefit from further validation through experiments.

426

427

428 **Supporting Information**

429

430 Cartesian coordinates for DFT-optimized structures.

431

432 **Author information**

433

434 ORCID

435 Christopher Parks: [0000-0001-8016-474X](https://orcid.org/0000-0001-8016-474X)

436

437 **Conflicts of interest**

438

439 The authors declare no competing financial interest.

440

441 The work described in this paper was funded by the ACT ALIGN CCUS Project No 271501.

442 This project has received funding from RVO (NL), FZJ/PtJ (DE), Gassnova (NO), UEFISCDI

443 (RO), BEIS (UK) and is co-funded by the European Commission under the Horizon 2020

444 programme ACT, Grant Agreement No 691712”

445

446 **Abbreviations:**

447 AHEIA - N-(2-aminoethyl)-N'-(2-hydroxyethyl)imidazolidin-2-one)

448 BHEEDA - N,N'-bis(2-hydroxyethyl)ethylenediamine

449 BHEOX - N,N'-bis(2-hydroxyethyl)

450 DEA – Diethanolamine

451 HEEDA - N-(2-hydroxyethyl)Ethylenediamine

452 HEF - N-(2-hydroxyethyl)-formamide

453 HEA - N-(2-hydroxyethyl)-acetamide

454 HEGly - N-(2-hydroxyethyl)glycine

455 HEI - N-(2-hydroxyethyl)imidazole
456 HHEA - 2-hydroxy-N-(2-hydroxyethyl)acetamide (HHEA)
457 HEIA - 1-(2-hydroxyethyl)imidazolidone
458 MAE - (2-Methylamino)ethanol
459 MEA – Monoethanolamine
460 OZD – Oxazolidinone

461

462 **References**

463

- 464 1. Kerr, R. A., Climate change. Global warming is changing the world. *Science* **2007**, *316* (5822),
465 188-190.
- 466 2. Dai, N.; Mitch, W. A., Effects of Flue Gas Compositions on Nitrosamine and Nitramine
467 Formation in Postcombustion CO₂ Capture Systems. *Environmental Science & Technology* **2014**, *48*
468 (13), 7519-7526.
- 469 3. Fine, N. A.; Goldman, M. J.; Rochelle, G. T., Nitrosamine Formation in Amine Scrubbing at
470 Desorber Temperatures. *Environmental Science & Technology* **2014**, *48* (15), 8777-8783.
- 471 4. Kim, J.; Lin, L.-C.; Swisher, J. A.; Haranczyk, M.; Smit, B., Predicting Large CO₂ Adsorption in
472 Aluminosilicate Zeolites for Postcombustion Carbon Dioxide Capture. *Journal of the American*
473 *Chemical Society* **2012**, *134* (46), 18940-18943.
- 474 5. Creamer, A. E.; Gao, B., Carbon-Based Adsorbents for Postcombustion CO₂ Capture: A Critical
475 Review. *Environmental Science & Technology* **2016**, *50* (14), 7276-7289.
- 476 6. Goepfert, A.; Czaun, M.; May, R. B.; Prakash, G. K. S.; Olah, G. A.; Narayanan, S. R., Carbon
477 Dioxide Capture from the Air Using a Polyamine Based Regenerable Solid Adsorbent. *Journal of the*
478 *American Chemical Society* **2011**, *133* (50), 20164-20167.
- 479 7. Jiang, Y.; Shi, X.-C.; Tan, P.; Qi, S.-C.; Gu, C.; Yang, T.; Peng, S.-S.; Liu, X.-Q.; Sun, L.-B.,
480 Controllable CO₂ Capture in Metal–Organic Frameworks: Making Targeted Active Sites Respond to
481 Light. *Industrial & Engineering Chemistry Research* **2020**, *59* (50), 21894-21900.
- 482 8. Manuilova, A.; Koiwanit, J.; Piewkhaow, L.; Wilson, M.; Chan, C. W.; Tontiwachwuthikul, P.,
483 Life Cycle Assessment of Post-combustion CO₂ Capture and CO₂-Enhanced Oil Recovery Based on the
484 Boundary Dam Integrated Carbon Capture and Storage Demonstration Project in Saskatchewan.
485 *Energy Procedia* **2014**, *63*, 7398-7407.
- 486 9. Kohl, A. L.; Nielsen, R. B., *Gas Purification*, . 5th ed. ed.; Elsevier Houston, TX: 1997.

- 487 10. Kennard, M. L.; Meisen, A., Gas chromatographic technique for analysing partially degraded
488 diethanolamine solutions. *Journal of Chromatography A* **1983**, *267*, 373-380.
- 489 11. Hsu, C. S.; Kim, C. J., Diethanolamine (DEA) degradation under gas-treating conditions.
490 *Industrial & Engineering Chemistry Product Research and Development* **1985**, *24* (4), 630-635.
- 491 12. Zhou, S.; Chen, X.; Nguyen, T.; Voice, A. K.; Rochelle, G. T., Aqueous Ethylenediamine for CO₂
492 Capture. *ChemSusChem* **2010**, *3* (8), 913-918.
- 493 13. Wang, Z.; Fang, M.; Pan, Y.; Yan, S.; Luo, Z., Amine-based absorbents selection for CO₂
494 membrane vacuum regeneration technology by combined absorption–desorption analysis. *Chemical*
495 *Engineering Science* **2013**, *93*, 238-249.
- 496 14. Li, J.; Henni, A.; Tontiwachwuthikul, P., Reaction Kinetics of CO₂ in Aqueous Ethylenediamine,
497 Ethyl Ethanolamine, and Diethyl Monoethanolamine Solutions in the Temperature Range of 298–313
498 K, Using the Stopped-Flow Technique. *Industrial & Engineering Chemistry Research* **2007**, *46* (13),
499 4426-4434.
- 500 15. Chakma, A.; Meisen, A., Identification of methyl diethanolamine degradation products by gas
501 chromatography and gas chromatography-mass spectrometry. *Journal of Chromatography A* **1988**,
502 *457*, 287-297.
- 503 16. Puxty, G.; Rowland, R.; Allport, A.; Yang, Q.; Bown, M.; Burns, R.; Maeder, M.; Attalla, M.,
504 Carbon Dioxide Postcombustion Capture: A Novel Screening Study of the Carbon Dioxide Absorption
505 Performance of 76 Amines. *Environmental Science & Technology* **2009**, *43* (16), 6427-6433.
- 506 17. Rao, A. B.; Rubin, E. S., A Technical, Economic, and Environmental Assessment of Amine-Based
507 CO₂ Capture Technology for Power Plant Greenhouse Gas Control. *Environmental Science &*
508 *Technology* **2002**, *36* (20), 4467-4475.
- 509 18. Polderman, L. D.; Dillon, C. P.; Steele, A. B., Why monoethanolamine solution breaks down in
510 gas-treating service. *Oil Gas J.* **1955**, *54*, 180–183.
- 511 19. Kim, C. J.; Sartori, G., Kinetics and mechanism of diethanolamine degradation in aqueous
512 solutions containing carbon dioxide. *International Journal of Chemical Kinetics* **1984**, *16* (10), 1257-
513 1266.
- 514 20. Davis, J.; Rochelle, G., Thermal degradation of monoethanolamine at stripper conditions.
515 *Energy Procedia* **2009**, *1* (1), 327-333.
- 516 21. Goff, G. S.; Rochelle, G. T., Monoethanolamine Degradation: O₂ Mass Transfer Effects under
517 CO₂ Capture Conditions. *Industrial & Engineering Chemistry Research* **2004**, *43* (20), 6400-6408.
- 518 22. Supap, T.; Idem, R.; Veawab, A.; Aroonwilas, A.; Tontiwachwuthikul, P.; Chakma, A.; Kybett,
519 B. D., Kinetics of the Oxidative Degradation of Aqueous Monoethanolamine in a Flue Gas Treating
520 Unit. *Industrial & Engineering Chemistry Research* **2001**, *40* (16), 3445-3450.

- 521 23. Rooney, P. C.; Dupart, M. S.; Bacon, T., Oxygen's role in alkanolamine degradation.
522 *Hydrocarbon Processing* **1998**, *77*, 109-113.
- 523 24. Chi, S.; Rochelle, G. T., Oxidative Degradation of Monoethanolamine. *Industrial & Engineering*
524 *Chemistry Research* **2002**, *41* (17), 4178-4186.
- 525 25. Fredriksen, S. B.; Jens, K.-J., Oxidative Degradation of Aqueous Amine Solutions of MEA, AMP,
526 MDEA, Pz: A Review. *Energy Procedia* **2013**, *37*, 1770-1777.
- 527 26. Gouedard, C.; Picq, D.; Launay, F.; Carrette, P. L., Amine degradation in CO₂ capture. I. A
528 review. *International Journal of Greenhouse Gas Control* **2012**, *10*, 244-270.
- 529 27. Lepaumier, H.; Picq, D.; Carrette, P.-L., New Amines for CO₂ Capture. II. Oxidative Degradation
530 Mechanisms. *Industrial & Engineering Chemistry Research* **2009**, *48* (20), 9068-9075.
- 531 28. Lawal, O.; Bello, A.; Idem, R., - Pathways and reaction products for the oxidative degradation
532 of CO₂ loaded and concentrated aqueous MEA and MEA/MDEA mixtures during CO₂ absorption from
533 flue gases. In *Greenhouse Gas Control Technologies 7*, Rubin, E. S.; Keith, D. W.; Gilboy, C. F.; Wilson,
534 M.; Morris, T.; Gale, J.; Thambimuthu, K., Eds. Elsevier Science Ltd: Oxford, 2005; pp 1159-1164.
- 535 29. Lawal, O.; Bello, A.; Idem, R., The Role of Methyl Diethanolamine (MDEA) in Preventing the
536 Oxidative Degradation of CO₂ Loaded and Concentrated Aqueous Monoethanolamine (MEA)-MDEA
537 Blends during CO₂ Absorption from Flue Gases. *Industrial & Engineering Chemistry Research* **2005**, *44*
538 (6), 1874-1896.
- 539 30. Strazisar, B. R.; Anderson, R. R.; White, C. M., Degradation Pathways for Monoethanolamine
540 in a CO₂ Capture Facility. *Energy & Fuels* **2003**, *17* (4), 1034-1039.
- 541 31. Bello, A.; Idem, R. O., Pathways for the Formation of Products of the Oxidative Degradation of
542 CO₂-Loaded Concentrated Aqueous Monoethanolamine Solutions during CO₂ Absorption from Flue
543 Gases. *Industrial & Engineering Chemistry Research* **2005**, *44* (4), 945-969.
- 544 32. Supap, T.; Idem, R.; Tontiwachwuthikul, P.; Saiwan, C., Analysis of Monoethanolamine and
545 Its Oxidative Degradation Products during CO₂ Absorption from Flue Gases: A Comparative Study of
546 GC-MS, HPLC-RID, and CE-DAD Analytical Techniques and Possible Optimum Combinations. *Industrial*
547 *& Engineering Chemistry Research* **2006**, *45* (8), 2437-2451.
- 548 33. Vevelstad, S. J.; Eide-Haugmo, I.; da Silva, E. F.; Svendsen, H. F., Degradation of MEA; a
549 theoretical study. *Energy Procedia* **2011**, *4*, 1608-1615.
- 550 34. Saeed, I. M.; Lee, V. S.; Mazari, S. A.; Si Ali, B.; Basirun, W. J.; Asghar, A.; Ghalib, L.; Jan, B. M.
551 Thermal degradation of aqueous 2-aminoethylethanolamine in CO₂ capture; identification of
552 degradation products, reaction mechanisms and computational studies. *Chem.Cent. J.* 2017, *11*

- 553 35. Yoon, B.; Hwang, G. S., On the mechanism of predominant urea formation from thermal
554 degradation of CO₂-loaded aqueous ethylenediamine. *Physical Chemistry Chemical Physics* **2020**, *22*
555 (30), 17336-17343.
- 556 36. Yoon, B.; Stowe, H. M.; Hwang, G. S., Molecular mechanisms for thermal degradation of CO₂-
557 loaded aqueous monoethanolamine solution: a first-principles study. *Physical Chemistry Chemical*
558 *Physics* **2019**, *21* (39), 22132-22139.
- 559 37. Xie, H.-B.; He, N.; Song, Z.; Chen, J.; Li, X., Theoretical Investigation on the Different Reaction
560 Mechanisms of Aqueous 2-Amino-2-methyl-1-propanol and Monoethanolamine with CO₂. *Industrial*
561 *& Engineering Chemistry Research* **2014**, *53* (8), 3363-3372.
- 562 38. M. J. Frisch; G. W. Trucks; H. B. Schlegel; G. E. Scuseria; M. A. Robb; J. R. Cheeseman; G.
563 Scalmani; V. Barone; B. Mennucci; G. A. Petersson; H. Nakatsuji; M. Caricato; X. Li; H. P. Hratchian;
564 A. F. Izmaylov; J. Bloino; G. Zheng; J. L. Sonnenberg; M. Hada; M. Ehara; K. Toyota; R. Fukuda; J.
565 Hasegawa; M. Ishida; T. Nakajima; Y. Honda; O. Kitao; H. Nakai; T. Vreven; J. A. Montgomery, J.; J.
566 E. Peralta; F. Ogliaro; M. Bearpark; J. J. Heyd; E. Brothers; K. N. Kudin; V. N. Staroverov; T. Keith;
567 R. Kobayashi; J. Normand; K. Raghavachari; A. Rendell; J. C. Burant; S. S. Iyengar; J. Tomasi; M.
568 Cossi; N. Rega; J. M. Millam; M. Klene; J. E. Knox; J. B. Cross; V. Bakken; C. Adamo; J. Jaramillo; R.
569 Gomperts; R. E. Stratmann; O. Yazyev; A. J. Austin; R. Cammi; C. Pomelli, J. W. O.; R. L. Martin; K.
570 Morokuma; V. G. Zakrzewski; G. A. Voth; P. Salvador; J. J. Dannenberg; S. Dapprich; A. D. Daniels;
571 O. Farkas; J. B. Foresman; J. V. Ortiz; J. Cioslowski; Fox, D. J. *Gaussian 09*, 2016.
- 572 39. Becke, A. D., Density-functional exchange-energy approximation with correct asymptotic
573 behavior. *Physical Review A* **1988**, *38* (6), 3098-3100.
- 574 40. Lee, C.; Yang, W.; Parr, R. G., Development of the Colle-Salvetti correlation-energy formula
575 into a functional of the electron density. *Physical Review B* **1988**, *37* (2), 785-789.
- 576 41. Perdew, J. P.; Chevary, J. A.; Vosko, S. H.; Jackson, K. A.; Pederson, M. R.; Singh, D. J.; Fiolhais,
577 C., Atoms, molecules, solids, and surfaces: Applications of the generalized gradient approximation for
578 exchange and correlation. *Physical Review B* **1992**, *46* (11), 6671-6687.
- 579 42. Dunning Jr., T. H., Gaussian basis sets for use in correlated molecular calculations. I. The atoms
580 boron through neon and hydrogen. *The Journal of Chemical Physics* **1989**, *90* (2), 1007-1023.
- 581 43. Parks, C.; Alborzi, E.; Akram, M.; Pourkashanian, M., DFT Studies on Thermal and Oxidative
582 Degradation of Monoethanolamine. *Industrial & Engineering Chemistry Research* **2020**, *59* (34),
583 15214-15225.
- 584 44. Galano, A.; Alvarez-Idaboy, J. R., Kinetics of radical-molecule reactions in aqueous solution: A
585 benchmark study of the performance of density functional methods. *Journal of Computational*
586 *Chemistry* **2014**, *35* (28), 2019-2026.

- 587 45. Mangiatordi, G. F.; Brémond, E.; Adamo, C., DFT and Proton Transfer Reactions: A Benchmark
588 Study on Structure and Kinetics. *Journal of Chemical Theory and Computation* **2012**, *8* (9), 3082-3088.
- 589 46. Scalmani, G.; Frisch, M. J., Continuous surface charge polarizable continuum models of
590 solvation. I. General formalism. *The Journal of Chemical Physics* **2010**, *132* (11), 114110.
- 591 47. Cossi, M.; Barone, V., Analytical second derivatives of the free energy in solution by polarizable
592 continuum models. *The Journal of Chemical Physics* **1998**, *109* (15), 6246-6254.
- 593 48. Grimme, S.; Ehrlich, S.; Goerigk, L., Effect of the damping function in dispersion corrected
594 density functional theory. *Journal of Computational Chemistry* **2011**, *32* (7), 1456-1465.
- 595 49. Cancès, E.; Mennucci, B.; Tomasi, J., A new integral equation formalism for the polarizable
596 continuum model: Theoretical background and applications to isotropic and anisotropic dielectrics.
597 *The Journal of Chemical Physics* **1997**, *107* (8), 3032-3041.
- 598 50. Funes-Ardoiz, I.; Paton, R. S. GoodVibes: Version 2.0.3. Zenodo 2018.
- 599 51. Zhao, Y.; Truhlar, D. G., The M06 suite of density functionals for main group thermochemistry,
600 thermochemical kinetics, noncovalent interactions, excited states, and transition elements: two new
601 functionals and systematic testing of four M06-class functionals and 12 other functionals. *Theoretical*
602 *Chemistry Accounts* **2008**, *120* (1), 215-241.
- 603 52. Petryaev, E. P.; Pavlov, A. V.; Shadyro, O. I., Homolytic deamination of amino alcohols. *J. Org.*
604 *Chem.* **1984**, *20*, 25-29.
- 605 53. Bedell, S. A., Oxidative degradation mechanisms for amines in flue gas capture. *Energy*
606 *Procedia* **2009**, *1* (1), 771-778.
- 607 54. Bedell, S. A.; Worley, C. M.; Darst, K.; Simmons, K., Thermal and oxidative disproportionation
608 in amine degradation—O₂ stoichiometry and mechanistic implications. *International Journal of*
609 *Greenhouse Gas Control* **2011**, *5* (3), 401-404.
- 610 55. Vevelstad, S. J.; Grimstvedt, A.; Elnan, J.; da Silva, E. F.; Svendsen, H. F., Oxidative degradation
611 of 2-ethanolamine: The effect of oxygen concentration and temperature on product formation.
612 *International Journal of Greenhouse Gas Control* **2013**, *18*, 88-100.
- 613 56. A. Katsuura; N. Washio Preparation of imidazoles from imines and iminoacetaldehydes. 2005.

614

615

616

617